specimen abuts a material of organic glass type on the other side. The physicomechanical characteristics for copper were taken exactly as in the previous computations, and for organic glass as: $\rho_0 = 1.2$ g/cm^3, $K = 8.95$ GPa, $G = 0.96$ GPa. The present solution with the rupture process taken into account is denoted by 1 in Fig. 6, without taking rupture into account by 3, experimental data [6] by 2, and numerical data [6] by dashes. The rise in stress around 0.8 μsec is explained by the arrival of a disturbance at the interface between the copper and the organic glass which is due to the origination and growth of pores in the target. Results of solving this problem agree qualitatively and in order of magnitude with the results in [6], which can also be considered as confirmation of the rupture model being used. Existing discrepancies, particularly the time shift, can be explained by differences in either the target thickness or the properties of the material.

LITERATURE CITED

1. V. S. Nikiforovskii and E. I. Shemyakin, Dynamic Rupture of Solids [in Russian], Nauka, Novosibirsk (1979).
2. A. I. Ruzanov, "Numerical modeling of solid body rupture under pulse loads," in: Applied Problems of Strength and Plasticity. Statics and Dynamics of Deformable Systems [in Russian], Gorkii State Univ. (1980).
3. T. W. Barbee, L. Seaman, et al., "Dynamic fracture criteria for ductile and brittle metals," J. Mater., 7, No. 3 (1972).
4. L. Seaman, D. R. Currand, and D. A. Shockey, "Computational models for ductile and brittle fracture," J. Appl. Phys., 47, No. 11 (1976).
5. J. H. Smith, "Three low-pressure spall thresholds in copper," in: Sympos. Dynam. Behavior Matter, Albuquerque, N. M., 1962. Amer. Soc. Test. and Mater. Philadelphia, Pa. (1963).
6. L. Seaman, "Effects of fracture on stress–strain relations for wave propagation," in: Materials of Second Sympos. Nonlinear Strain Waves [in Russian], Inst. Kibern. Akad. Nauk ESSR, Tallin (1978).
7. S. A. Novikov, I. I. Divnov, and A. G. Ivanov, "Investigation of the rupture of steel, aluminum, and copper under explosive loading," Fiz. Met. Metalloved., 21, No. 4 (1966).
8. G. V. Stepanov, Elastic–Plastic Strain of Materials Subjected to Pulse Loads [in Russian], Naukova Dumka, Kiev (1979).
9. S. Cochran and D. Banner, "Spall studies in uranium," J. Appl. Phys., 48, No. 7 (1977).

LIMITING STRAINS OF THE DYNAMIC FRACTURE OF CYLINDRICAL SHELLS

V. V. Selivanov

UDC 399.374.1

The implementation of the fracture criteria of [1, 2] with application to rigidly plastic cylindrical shells expanding under the action of detonation products is discussed. The experimental results for the determination of the limiting strains of the shells are discussed. The problem of the limiting strains of cylindrical shells under the action of detonation products expanding in equilibrium has been discussed in [2-4]. Numerical and analytic solutions describing the process of deformation of a cylindrical rigidly plastic shell have been obtained in [4, 5].

We shall consider some criteria and conditions for the fracture of rigidly plastic shells. An outer zone with a mixed stress state ($\sigma_r < 0$, $\sigma_\theta > 0$) and an inner zone in which a state of hydrostatic equilibrium ($\sigma_r < 0$, $\sigma_\theta < 0$) is realized arise in a cylindrical shell acted on by an intense internal load [4]. Here σ_r and σ_θ are the radial and tangential components of the stress tensor. The condition satisfied on the boundary of both zones has the form $\sigma_\theta = 0$. Its use together with the plasticity condition ($\sigma_\theta - \sigma_r = \varkappa Y$) and the expression for the radial stress [5] in the initial position ($a = a_0$, $b = b_0$) will give the coordinate of the boundary $\sigma_\theta = 0$:

Moscow. Translated from Zhurnal Prikladnoi Mekhaniki i Tekhnicheskoi Fiziki, No. 4, pp. 122-127, July-August, 1982. Original article submitted June 24, 1981.

0021-8944/82/2304-0574$07.50

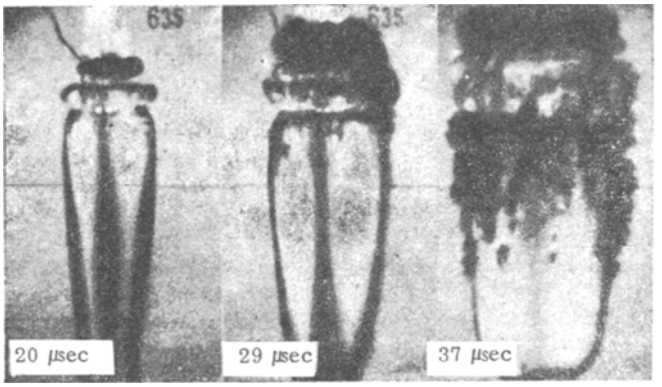

Fig. 1.

$$r = b_0 (b_0/a_0)^{-\varkappa Y/p_0}. \tag{1}$$

Here b_0 and a_0 are the initial outer and inner radii of the shell, Y is the dynamic yield point ($\varkappa = 2/\sqrt{3}$) for the von Mises–Henke plasticity condition, $\varkappa = 1$ for the St. Venant–Tresk plasticity condition), and $p_0 = \rho_0 D^2/2(k+1)$ is the pressure of instantaneous detonation (ρ_0, explosives density; D, detonation velocity; and k, polytropic index).

In the case of spherical symmetry and in the general case of motion of a shell ($a > a_0$, $b > b_0$) analogous calculations result in a transcendental equation which has no analytic solutions. However, analysis of the results of a numerical solution [4] and linearization of the equation $\sigma_r = f(a_0, a, b_0, b, r, p_0, Y, \varkappa)$ [5] indicate that the stress distribution over the shell thickness can be assumed to be linear. Then in accordance with [2] the fracture radius of the inner surface is determined by the expression [4]

$$a_f = a_0 (p_0/Y)^{1/2k}. \tag{2}$$

Taking account of simultaneous fracture by shear [3], we obtain

$$a_f^0 = a_0 (2p_0/Y)^{1/2k}. \tag{3}$$

For fixed values of p_0, Y, and k = 3 the ratio $a_f^0/a_f = 1.12$ in the case of cylindrical symmetry and $a_f^0/a_f = 1.08$ in the case of spherical symmetry.

Optical photographs made in reflected light of shells loaded by the detonation products of explosive charges have shown that it is necessary to distinguish between the radius of formation of cracks on the outer surface b_c and the fracture radius b_f, which is fixed by the breakthrough of detonation products to the outer surface. Some experimental results for Armco iron are presented in Fig. 1. The experimental values of the relative radii of brack formation b_c/b_0 and fracture radius b_f/b_0 are presented in Table 1 (the shell dimensions are a_0 = 10 mm, b_0 = 13.5 mm, length l_0 = 130 mm, bottom thickness 10 mm, and cover thickness 5 mm). The shells were loaded by the detonation products of a TG 50/50 charge with a density of $1.65 \cdot 10^3$ kg/m^3, a detonation velocity of $7.6 \cdot 10^3$ m/sec, and an instantaneous detonation pressure of $119 \cdot 10^8$ Pa. The shell material is made out of carbon iron alloys with different heat treatment (1 — hardening with low annealing and 2 — hardening with high annealing) and with plastic properties: static yield point σ_y and relative construction upon tension ψ. The calculated values of the fracture radii according to the relationship (2) using the static ($b_f^{(1)}/b_0$) and dynamic ($b_f^{(2)}/b_0$) yield points are given here. The dynamic yield point was determined from the static value with the experimental results of [6] taken into account.

It is evident that the fracture radii determined from the dependence (2) do not correspond to the experimental values. This circumstance is explained by the fact that Taylor's hypothesis [2] proposes the presence of an outer fractured zone of the shell (1) prior to the start of its motion. Physically, this invalid premise results in a decrease in the calculated values of b_f/b_0 which correspond more closely to the crack formation radii (b_c/b_0), and the use of the static yield point gives the best results for relatively plastic materials, as does the use of the dynamic yield point for relatively brittle materials.

We shall consider a fraction criterion of the type $\varepsilon_i^* = \varepsilon_{i_t} f(\Pi)$ [1], where ε_i^* is the critical strain intensity at which fracture of the material occurs, ε_{i_t} is the degree of

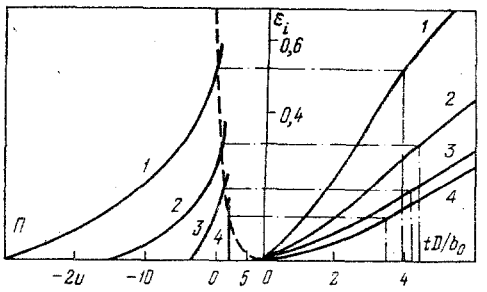

Fig. 2.

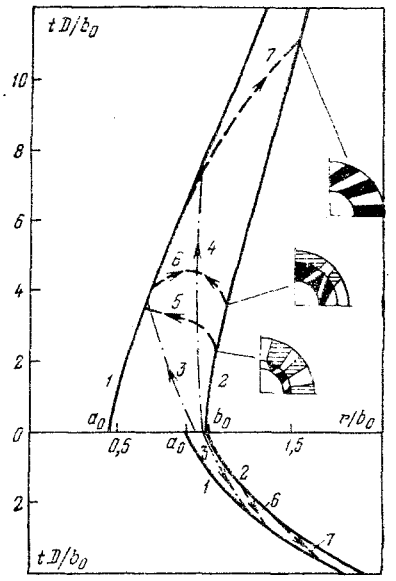

Fig. 3.

deformation up to the instant of rupture in the case of tension, and $\Pi = 3\sigma/\sigma_i$ is the stiffness coefficient of the stress state (σ is the average stress, and σ_i is the stress intensity).

In the case of a cylindrical shell $\Pi = 3\sigma_r/Y + 1.734$ for the von Mises condition, from which it follows that on the outer surface of the shell ($\sigma_r = 0$) $\Pi = 1.734$ and on the inner surface ($\sigma_r = -p$) $\Pi = -3p/Y + 1.734$. This corresponds to a state of hydrostatic pressure right up to the value $p/Y = 0.578$, after which a state of tension occurs.

The strain intensity in any cross section of a cylindrical shell is determined, according to [5], from the expression $\varepsilon_i = -(1/\sqrt{3}) \ln (1 - (a^2 - a_0^2)/r^2)$, from which it follows that on the outer shell surface $\varepsilon_i = -(2/\sqrt{3}) \ln (b_0/b)$ and on the inner surface $\varepsilon_i = -(2/\sqrt{3}) \ln (a_0/a)$, where r is the Eulerian coordinate.

The experimental dependence

$$\varepsilon^* = 2\varepsilon_{i_t} e^{-0.72\Pi} \tag{4}$$

has been proposed in [1] for stamping processes. We note that in the case of uniaxial tension ($\Pi = 1$) $\varepsilon_i^* \approx \varepsilon_{i_t}$.

The construction of a fracture surface for cylindrical shells consists of the calculation of the instantaneous stress–strain state of the shell [4, 5] and the graphical implementation of the dependences $\varepsilon_i(\bar{t})$ and $\Pi(\bar{t})$ in various cross sections of the shell ($\bar{t} = tD/b_0$). The intersection of the exponential function (4) with the corresponding curves $\varepsilon_i(\Pi)$ gives the time and strain of the fracture of a fixed cross section of the shell.

A nomogram for a shell with $a_0/b_0 = 0.446$, $\varepsilon_{i_t} = 0.25$ ($\psi = 0.22$), and $\sigma_y \approx 7 \cdot 10^8$ Pa ($Y \approx 14 \cdot 10^8$ Pa) is given in Fig. 2 according to the results of the numerical solution of [4]. Curves 1-4 refer to Lagrangian particles of the shell with the initial coordinates $r_0 = 0.446$, 0.667, 0.889, and 1.0, respectively. An approximate relationship between ε_{i_t} and ψ is of the form $\varepsilon_{i_t} \approx \ln [1/(1 - \psi)]$.

Similar dependences are constructed for plastic ($\varepsilon_{i_t} = 1$) and brittle ($\varepsilon_{i_t} = 0.1$) materials as well as for a shell with $a_0/b_0 = 0.871$, $\varepsilon_{i_t} = 0.25$, and $\varepsilon_{i_t} = 1$.

The r–t diagrams of the expansion and fracture processes of shells with $a_0/b_0 = 0.446$ (upper half-plane) and $a_0/b_0 = 0.871$ (lower half-plane) are given in Fig. 3. The motion of fracture surfaces according to the criterion (4) is denoted by the dashed lines, and motion according to Taylor's dependence (1) is denoted by the dash–dotted lines; the arrows indicate the direction of motion of the fracture front. Here 1 and 2 indicate the laws of motion of the surface boundary $\sigma_\theta = 0$ for $Y = 10^8$ and 10^9 Pa, respectively, and 5-7 indicate the laws of motion of the fracture front according to the criterion (4) for $\varepsilon_{i_t} = 0.1$, 0.25, and 1, respectively.

TABLE 1

Shell material	Kind of heat treatment	$\sigma_y \times 10^{-8}$, Pa	ψ	b_c/b_0	b_f/b_0	$b_f^{(1)}/b_0$	$b_f^{(2)}/b_0$	$b_f^{(3)}/b_0$
Steel 60	1	7,0	0,25	1,26	1,49	1,36	1,24	1,43
" 60	2	5,5	0,4	1,40	1,88	1,41	1,25	1,68
" 45Kh	1	9,0	0,3	1,25	1,50	1,32	1,23	1,46
" 45Kh	2	6,0	0,4	1,35	1,87	1,39	1,25	1,68
" 35		3,2	0,45	1,41	1,91	1,51	1,28	1,74
Armco iron		1,2	0,85	2,1	2,8	1,78	1,36	2,58
VCh-60-2 cast iron		—	0,03	1,12	1,37	—	—	1,34

As has been noted above, according to the criteria (2) and (3), there is a fractured zone in the shell at t = 0 which is adjacent to the outer surface. This contradicts the energy conservation law and finds no experimental confirmation. In addition the dependences (2) and (3) lead to an unambiguous increase in the fracture radius when the yield point decreases, which is not obligatory in the general case and contradicts the experimental results (Table 1) in a number of cases.

A criterion which takes account of a relation of the form of stress state II with the limiting strain intensity ε_i^* of (4) and which has a number of singularities is the most plausible. If the fracture always propagates from the outer surface to the inner one for relatively thin-walled shells, then in the case of a thick-walled shell the development of the fracture surface is determined, other conditions being equal, by the plasticity of the material and can start both from the outer (brittle materials 5) and from the inner (plastic materials 7) surfaces, and for materials with intermediate plasticity 6 — from both sides, finishing in the middle zone of the shell (Fig. 3). The fracture radii were: for a_0/b_0 = 0.446 when ε_{it} = 0.1, b_f/b_0, = 1.11, ε_{it} = 0.25, b_f/b_0 = 1.17, and ε_{it} = 1, b_f/b_0 = 1.5, and for a_0/b_0 = 0.871 when ε_{it} = 0.25, b_f/b_0 = 1.46 and when ε_{it} = 1, b_f/b_0 = 1.6. We note that notwithstanding the various fracture times the limiting fracture strain of different shell cross sections (r_f/r_0) increases from the outer surface to the inner one, which is explained by a decrease in the stiffness of the stress state upon a shift from the outer surface (II > 0) to the inner one (II < 0). The limiting strains of different cross sections (r_f/r_0) and the fracture times ($t_f = t_f D/b_0$) are given in Table 2 for a shell with a_0/b_0 = 0.446.

The use of criterion (4) for the analysis of the fracture of rigidly plastic shells loaded by detonation products seems very promising. In the first place the fracture radii ($b_f^{(3)}/b_0$) calculated according to the procedure of [4] using the criterion (4) indicate satisfactory agreement between the experimental and theoretical results with an accuracy determined by the measurement error and the model of the problem (see Table 1). Secondly, the process of formation and propagation of a fracture front in shells with different plasticity corresponds to the experimental data and the fracture phenomenology. A combined discussion of the r—t diagram (see Fig. 3) and the stress—strain diagram of the state (see Fig. 2) permits giving a qualitative interpretation of the possible type of fracture. Thus for a

TABLE 2

ε_{it}	r_0	$\bar{t}_f$	r_f/r_0
0,1	0,446	3,3	1,48
	0,667	3,1	1,21
	0,889	2,9	1,11
	1,0	2,2	1,06
0,25	0,446	4,0	1,58
	0,667	4,5	1,37
	0,889	4,25	1,19
	1,0	3,5	1,12
1,0	0,446	6,8	2,06
	0,667	9,4	1,81
	0,889	10,6	1,58
	1,0	11,0	1,5

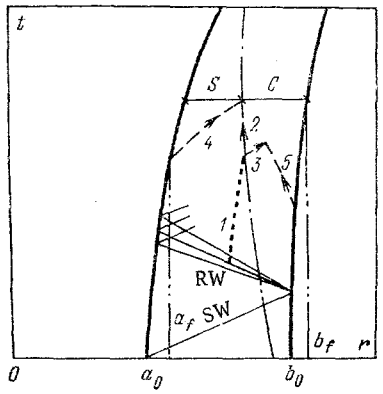

Fig. 4.

thick-walled shell ($a_0/b_0 = 0.446$) the low plasticity ($\varepsilon_{it} = 0.1$) leads to a small deformation time of the material in the zone of hydrostatic nonuniform compression and predominant fracture by breaking away from the outer surface in the presence of a small shear zone on the inner shell surface. This is illustrated in Fig. 3, in which the cross section of fragments formed in connection with fracture by breaking away is denoted by the hatching, and by shear — by a dark background. When the plastic properties of the material ($\varepsilon_{it} = 0.25$) increases, the plastic flow time in the inner zone and the zone dimensions correspondingly increase, which, notwithstanding termination of the fracture process in a tension region, leads to predominant fracture by shear. Actually, fractography of the fracture surfaces indicates an increase in the relative fraction of viscous rupture (in %) under the indicated conditions. Upon a further increase in the plasticity of the material ($\varepsilon_{it} = 1.0$) the entire fracture process may be of a shear nature, although the relative fraction of viscous rupture increases along the direction to the outer surface and depends on the deformation time of the material in the hydrostatic compression zone ($\Pi < 0$).

Thirdly, the use of the criterion (4) permits applying it along with the wave criteria which determine the origin of cracks and fracture centers in the inner region of the shell due to the action of rarefaction waves. It has been noted in [7] that fracture in connection with longevity in the microsecond range is of a multisource nature with the formation of numerous spall centers and their subsequent merging into a main crack, i.e., fracture in this case is not controlled by plastic deformation. The subsequent development of the fracture process depends on the nature of the variation of the stress–strain state of the shell in the ballistic stage of separation. At the initial time one can use the solution of the deformation of a compressible elastoplastic shell [8, 9] and the criteria of spall strength [10] or the experimental results [11]. If centers of wave fracture (line 1, Fig. 4) appear in the rarefaction wave (RW) formed upon the reflection of a shock wave (SW) from a free surface, then their subsequent development is determined both by the motion of the line $\sigma_\theta = 0$ (dash–dotted line) and by attainment of the limiting strains in other cross sections of the shell. Migration of the tension zone into the region of wave fracture centers leads to the development of cracks inside the shell following the tension front (line 2), and a crack of brittle breaking away propagates with velocity c_f (line 3) towards the outer surface. Both fracture fronts meet the fronts formed on the inner (line 4) and outer (line 5) surfaces due to the realization of criterion (4). Then two fracture regions are formed — by shear S and by breaking away C; the direction and conditions of their propagation leads to differences in the structure of one type of crack discontinuity. The fracture radii of the inner surface a_f and the final fracture radius determined from the value of the outer fracture radius b_f are found by graphical means.

The analysis has been restricted to the particular case of the expansion of plastic shells. Such a restriction has an advantage in that the simplifications associated with the symmetry conditions permit applying to the treatment of some complicated problems a simple mathematical apparatus which is very difficult under other conditions.

LITERATURE CITED

1. G. A. Smirnov–Alyaev, Mechanical Principles of Plastic Working of Metals [in Russian], Mashinostroenie, Moscow (1968).

2. G. I. Taylor, Scientific Papers, Vol. 8, Cambr. Univ. Press, Cambridge (1963).
3. G. R. Hoggatt and R. F. Recht, "Fracture behavior of tubular bombs," J. Appl. Phys., 39, No. 3 (1968).
4. V. A. Odintsov, V. V. Selivanov, and L. A. Chudov, "The expansion of an ideally plastic cylindrical shell under the action of detonation products," Zh. Prikl. Mekh. Tekh. Fiz., No. 2 (1974).
5. V. A. Odintsov and V. V. Selivanov, "The behavior of a rigidly plastic cylindrical shell under the action of internal pressure," Zh. Prikl. Mekh. Tekh. Fiz., No. 3 (1975).
6. A. G. Ivanov, S. A. Novikov, and V. A. Sinitsyn, "An investigation of elastoplastic waves in iron and steel in connection with explosive loading," Fiz. Tverd. Tela, 5, No. 1 (1963).
7. N. A. Zlatin, G. S. Pugachev, et al., "The temporal dependence of the strength of metals in connection with longevities of the microsecond range," Fiz. Tverd. Tela, 17, No. 9 (1975).
8. V. A. Odintsov, V. V. Selivanov, and L. A. Chudov, "The motion of an elastoplastic shell with a phase transition under the action of detonation products," Mekh. Tverd. Tela, No. 3 (1974).
9. V. A. Odintsov, V. V. Selivanov, and L. A. Chudov, "The expansion of a thick-walled cylindrical shell under the action of an explosive load," Mekh. Tverd. No. 5 (1975).
10. G. V. Stepanov, Elastoplastic Deformation of Materials under the Action of Pulse Loads [in Russian], Naukova Dumka, Kiev (1979).
11. E. F. Gryaznov, V. A. Odintsov, and V. V. Selivanov, "Smooth annular fragments," Mekh. Tverd. Tela, No. 6 (1976).

PLASTIC DEFORMATIONS OF A CYLINDRICAL SHELL UNDER THE ACTION OF A PLANAR EXPLOSION WAVE

R. G. Yakupov

UDC 539.374

A thin-walled circular cylindrical shell of infinite length is located in the ground. At a specified distance from the shell a planar charge of explosive material, of infinite length along the direction of the cylinder axis, explodes, and a planar plastic shock wave develops in the medium. The wave front is parallel to the cylinder directrix, and the wave parameters are known. It is necessary to find the residual cylinder deformations as a function of explosion wave pressure.

We will locate the origin of a coordinate system y, w at the point O in the direction of the incident wave (Fig. 1a). We write the equations of motion of a shell element experiencing displacements of the order of the magnitude of the shell wall thickness in the form [1]

$$T' = N_y' = 0,\ M'' + ((1/R) + w'')N_y + q + q_1 - \rho H\ddot{w} = 0, \tag{1.1}$$

where T, N_y are the tangent and normal stresses in the mean surface; M_y, bending moment in the peripheral direction; R, H, radius and wall thickness of the shell; ρ, density of the material; w, radial displacement; q, q_1, pressure of the wave and the surrounding medium; the prime denotes differentiation with respect to y, and the dot, with respect to t.

Reflection of a planar plastic shock wave from a planar barrier at normal incidence and incidence at an angle has been studied in [2, 3]. To determine the explosion wave pressure on the shell, we will use the results of those studies and the "isolated element principle," according to which an incident plane wave is reflected from a curvilinear boundary in the vicinity of each point just as it is reflected from a small element of a plane passing through the given point. We write the expression for wave pressure in the form

$$q = p_0(1 - t/t_0)\cos\theta,\ -\pi/2 \leqslant \theta \leqslant \pi/2,\ t > 0,\ q = 0,\quad \pi/2 \leqslant \theta \leqslant -\pi/2, \tag{1.2}$$

where $p_0 = p_{1*}(1 + \sqrt{n})$; p_{1*} is the pressure on the incident wave front at the moment of

Ufa. Translated from Zhurnal Prikladnoi Mekhaniki i Tekhnicheskoi Fiziki, No. 4, pp. 127-132, July-August, 1982. Original article submitted June 26, 1981.

